Ultrasonics Sonochemistry 90 (2022) 106180

Contents lists available at ScienceDirect

Ultrasonics Sonochemistry

journal homepage: www.elsevier.com/locate/ultson

A rapid synthesis of nanofibrillar cellulose/polystyrene composite via ultrasonic treatment

K.A. Cherednichenko [a], A.R. Sayfutdinova [a], A. Kraynov [a], B. Anikushin [a], V. Ignatiev [a], M.I. Rubtsova [a], S.A. Konstantinova [a], D.G. Shchukin [b,*], V.A. Vinokurov [a]

[a] National University of Oil and Gas «Gubkin University», Moscow 119991, Russia
[b] Stephenson Institute for Renewable Energy, Department of Chemistry, University of Liverpool, Liverpool L69 7ZD, United Kingdom

A B S T R A C T

A new method of the synthesis of nanofibrillar cellulose/polystyrene composite based on ultrasonic treatment of styrene emulsion in cellulose-water solution was elaborated. A new approach does not require additional heating and proposes a significantly faster synthesis (15 min, 45 °C) of the target composite compared to the methods described previously. A comprehensive analysis did not reveal any significant differences between mechanical, physical and biodegradable properties of the composite obtained by ultrasonic method and that one obtained by conventional thermal method, which requires much higher temperature (above 75 °C) and reaction duration (from 3 h).

1. Introduction

Cellulose is a natural polymer attracting considerable attention of researches all over the world owing to its abundance and hence low price, renewable and biodegradable feedstock as well as its outstanding mechanical properties and high aspect ratio [1,2]. Since cellulose is the main reinforcing phase in plants, its fibers can be extracted from various plant sources (wood, wheat straw, cotton, hemp, etc.) by the mechanical treatment of cellulose pulp [2,3]. The obtained microfibrillar cellulose (MFC) consists of aggregates of cellulose microfibrils. The individual microfibril is several tens of microns in length and 20–40 nm in thickness and has heterogeneous structure and morphology alternating crystalline and amorphous regions [3]. Following acidic, mechanical or enzymatic treatment leads to further transverse cleavage of microfibrils along the amorphous regions resulting in nano-scaled crystalline fibers [4,5]. The employment of the chemical and enzymatic treatment of cellulose fibers to get cellulose nanocrystals (CNCs) and cellulose nanofibrils (CNFs) helped to overcome problem of high energy consumption (during long mechanical treatment) and, thus, to reduce their price. Nanofibrillated cellulose possesses outstanding mechanical, chemical and physical properties [6], that is why it seems to be an ideal biopolymer for the wide application in industry.

The application of cellulose as a matrix filler for different polymer additives is of great interest due to the potential of producing novel renewable, biodegradable composite materials with improved mechanical and physical properties [3]. The properties of cellulose/polymer composites significantly depend on cellulose content, as well as cellulose fiber size, aspect ratio, orientation and cellulose/matrix adhesion [3,7–9]. The latter is of great importance since mixing of the hydrophilic cellulose fibers with hydrophobic polymers (e.g., polypropylene, polyethylene, polystyrene, etc.) is energetically unfavorable from thermodynamic point of view [4,10–12]. A number of different approaches to mix hydrophilic cellulose with hydrophobic polymer have been considered the recent years. For instance, chemical modification of cellulose surface (grafting of polymers to cellulose surface, adsorption of surfactants onto fibrils, replacing hydroxyl groups with hydrophobic molecules) has been considered as an approach to improve its dispersion in polymer matrix [13–18]. However, chemical modification of cellulose leads to decrease of hydroxyl groups number on its surface resulting in weaker hydrogen bonding and, hence, worse mechanical properties of the final composite [3,10]. To overcome this disadvantage, a Pickering emulsion approach was developed recently [10,12,19,20]. In this approach, the corresponding monomer (e.g., styrene [10]) mixed with radical initiator was added to diluted cellulose water solution which acts as emulsifier to assist monomer solvation. The polymerization undergoes at stirring at moderate temperature (70 °C) during 12 h. The obtained composite particles were hot-pressed at 160 °C to get the final material. Despite homogeneous dispersion of cellulose fibers in polymer matrix, the described method has one significant drawback: the preparation of polystyrene (PS)/cellulose composite particles is rather time consuming. Slow diffusion of monomer/oligomer molecules in diluted cellulose water solution could be one of the reasons of such a long

* Corresponding author.
E-mail address: shchukin@liverpool.ac.uk (D.G. Shchukin).

https://doi.org/10.1016/j.ultsonch.2022.106180
Received 1 July 2022; Received in revised form 19 September 2022; Accepted 24 September 2022
Available online 26 September 2022

polymerization reaction time.

An acceleration of emulsion-type polymerization reaction can be achieved with help of ultrasonic irradiation [21]. Production of H· and HO· radicals during ultrasonic treatment can initiate polymerization of monomers in water solutions [22–24]. Polymer structure and, thus, its properties can be considerably controlled by the use of ultrasound [25]. Y. Kojima *et al.* [26] provided styrene polymerization at a wide range of frequencies: from 23.4 kHz to 1 MHz. The maximum acceleration of polymerization reaction was found at 23.4–92 kHz range, whereas no polymerization was observed at high frequencies (518 kHz and 1 MHz). Thus, the selection of optimum sonication frequency range is important to achieve the fastest polymerization rate.

In this work we synthesized nanofibrillar cellulose/polystyrene (NFC/PS) composite particles by employing modified Pickering emulsion approach [10]. In order to speed up styrene polymerization, the ultrasonic irradiation was applied during synthesis. Such modification has significantly accelerated polymerization rate: from 3 h to 15 min to complete reaction. The morphology of the obtained composite materials was investigated by scanning electron microscopy (SEM). The comprehensive studies of the obtained NFC/PS composites revealed considerable amelioration of physical, mechanical and biological properties compared to those of PS. No significant difference was observed between properties of both composites obtained by different ways, which validates the possibility to replace a long traditional synthetic procedure by the faster ultrasonic one.

2. Experimental

2.1. Raw materials

Softwood sulfate bleached pulp (GOST 9571–89) was received from Arkhangelsk Pulp and Paper Mill. Pulp characteristics are presented in Table S1, Supporting Information section. Styrene monomer, ammonium persulfate ($(NH_4)_2S_2O_8$, 97.0 %), sulphuric acid (H_2SO_4, 98 %) and hydrogen peroxide (H_2O_2, 37 %) were purchased from Sigma Aldrich.

2.2. NFC preparation

We employed a procedure described previously [27]. A moist cellulose pulp was washed in distilled water and filtered on a Buhner funnel for 3 times in order to remove traces of conservation solution. 19.5 g of moisture washed cellulose and 8.1 g of hydrogen peroxide were added to the sulphuric acid solution obtained by mixing 168.4 g of concentrated sulphuric acid and 104 g of distilled water. The resulting solution contained 2 wt% of cellulose, 1 wt% of hydrogen peroxide and 55 wt% of sulphuric acid was stirred in Biosan ES20/40 orbital shaker incubator at 600 rpm for 4 h. The stirring was followed by suspension filtration and washing with distilled water. The obtained precipitate was then dispersed in distilled water to get 3 wt% suspension using Branson Digital Sonifier 450 (20 kHz, 400 W) and homogenized by IRA Ultra-turrax T-18 digital homogenizer to get NFC in powder form.

2.3. NFC/PS composite particle synthesis

The obtained previously 3 wt% NFC suspension was mixed with styrene in 1000 ml flask at room temperature under intensive stirring. The final solution volume was 600 ml. The weight ratio of styrene/dry NFC was 1/1. The obtained solution was ultrasonically treated (20 kHz, 3.3 W/cm^2) during 3 min to get the better emulsion with increasing of the solution temperature to 40 °C. The emulsion droplets diameters were analyzed before and after ultrasonic treatment by light microscopy (Fig. S1). The average diameters of styrene droplets before and after ultrasonication are 101 ± 70 μm and 10 ± 5 μm, respectively. Then, two different procedures were employed to get NFC/PS composite particles.

According to the first procedure (***Procedure I***), the temperature of obtained emulsion was elevated to 70 °C and ammonium persulfate was added at constant stirring. The weight ratio of $(NH_4)_2S_2O_8$/styrene was set to 1/100. Styrene polymerization underwent at constant stirring at 75 °C in flask with a condenser. Reaction time was varied from 2 to 5 h. The obtained composite NFC/PS particles were filtered, washed 3 times with deionized water and dried at 60 °C for 24 h.

According to the second procedure (***Procedure II***), the NFC/styrene emulsion was sonicated using Branson Digital Sonifier 450 (20 kHz, 400 W) after $(NH_4)_2S_2O_8$ addition ($(NH_4)_2S_2O_8$/styrene ratio was the same as in ***Procedure I***). The solution temperature of 45 °C was maintained by thermal regulation through external water circuit during the whole procedure. Sonication time was varied from 5 to 20 min. The obtained NFC/PS precipitate was collected and dried in the same way as for the first procedure. The samples obtained with use of ultrasonic treatment was marked as NFC/PS/US in the paper for the convenience.

To prepare final composite, 0.5 g of composite particles was pressed for 15 min in a hand screw press with a force of up to 1 ton and heated to 230 °C. Resulted tablet samples were air cooled and had a diameter of 35 mm and a thickness of 0.5 mm.

2.4. Electron microscopy

Cellulose nanofibers as well NFC/PS particles were investigated by scanning electron microscopy (SEM) by JEOL JIB4501 multibeam system and transmission electron microscopy (TEM) by JEOL JEM2100 UHR.

The non-conductive samples for SEM investigation were placed on conductive carbon tape and coated by 15 nm gold layer using ion sputter coater Q150R ES Plus (Quorum Technologies ltd). The acceleration voltage was set to 10 kV range.

The diluted suspensions of NFC and NFC/PS were placed on carbon/formvar TEM Cu grids (TedPella, Inc.) and investigated at 200 kV acceleration voltage. The micrographs were acquired by Quemesa 11MegaPixel Olympus CDD camera.

The images were treated using ImageJ software [28,29].

2.5. Fourier-transform infrared spectroscopy

Fourier-transform infrared (FTIR) spectroscopy studies of NFC/PS composite samples were performed using Nicolet iS 10 FTIR Spectrometer (Thermo Scientific, USA) with germanium ATR crystals. The absorption mode spectra were collected in 600–4000 cm^{-1} range.

2.6. Thermogravimetric analysis

Thermogravimetric analysis (TGA) of the samples was carried out on STA 449 F5 Jupiter instrument (NETZSCH, Germany). 10 mg of NFC/PS composite was placed into a corundum crucible. The data were collected in the range from 25 h to 500 °C with a heating rate of 10 °C/min. The experiments were carried out under nitrogen atmosphere.

2.7. Micro-hardness test

Micro-hardness measurements of the obtained composite samples were performed using a Fischerscope HM2000 S nanoindenter. The load and displacement of the indenter under loading and unloading were measured. Every sample was subjected to series of loads in 0–300 mN range, the maximum force of 300 mN was reached in application time of 20 s, creep at maximum force was 5 s. Vikers hardness (H_V) and Martens hardness (H_M) were calculated based on load/displacement relationships.

2.8. Contact angle measurements

The three-phase contact angle of the samples was measured with help of Kruss DSA100. PS and composite sample were placed into the cuvette at saturated vapour condition. Then, 1.0 μL water droplet was

added onto a sample's surface and the contact angle was measured.

2.9. Biodegradability test

To estimate the potential of produced composites to biodegrade in the presence of microorganisms, bioresistance tests were made by exposure to mold fungi according to ISO 846 ASTM G 21–96 (Standard Practice for Determining Resistance of Synthetic Polymeric Materials to Fungi). *Aspergillus niger* Tiegh, *Aspergillus terreus* Thom, *Aspergillus jryzae (Ahlburg)* Cohn, *Chaetomiumglobosum* Kunze, *Paecilomyces varioti* Bainer, *Penicillium funiculosum* Thom, *Penicillium chrisogenum* Thom, *Penicillium cyclopium* Westling, *Trichoderma viride* Pers ex Fr were used as a testing microorganisms. Two types of experiments were carried out.

To investigate fungus resistance, sterile Petri dish with the composite samples and PS sample were inoculated in a suspension of fungal spores homogeneous distributed with a sprayer without allowing the droplets to coalesce. This method determines the fungal resistance of the materials and their components without mineral and organic contaminants.

To study fungicidal and fungistatic properties of the samples, sterile Petri dish was filled with Chapek-Dox agarized medium. Then, the composite samples as well as PS sample were placed in Petri dish and incubated the samples contaminated with mould spores in a solution of mineral salts with the addition of sucrose under conditions favourable for their growth and development.

In the both experiments sterile Petri dish filled with the composites without fungi was used as a benchmark. All Petri dishes were kept in the test chambers at a temperature of (29 ± 2)° C and greater than 90 % relative humidity. Duration of the both experiments (from the moment of the regime established) was 28 days. At the end of the tests, the samples were removed from the chamber and visually tested under a microscope. The intensity of mold fungus development was evaluated according to the six-point scale of ISO 846 ASTM G 21–96 presented below Table 1.

3. Discussion and results

To obtain NFC/PS composite particles, a modified procedure proposed by Y. Jang *et al.* [10] was employed. In our synthesis, the original regenerated cellulose was replaced by NFC. Styrene monomer addition to the aqueous solution containing 3 %wt of NFC led to immediate phase separation. However, a short ultrasonic treatment (3 min) provided a stable Pickering emulsion of styrene droplets in water. Analysis of optical micrographs of styrene droplets revealed their considerable shrinkage after ultrasonic treatment (Fig. S1). The average diameters of styrene droplets before and after ultrasonication are 101 ± 70 μm and 10 ± 5 μm respectively. Stability of the obtained emulsion was found to be significantly better than that of styrene-water solution without NFC due to cellulose adsorption at the monomer/solvent interface. The stabilization effect of NFC can be explained by the amphiphilic nature of cellulose: it has hydrophilic hydroxyl groups on its surface and hydrophobic glucopyranose rings [30,31].

PS polymerization led to the formation of white precipitate which was visually controlled to stop the reaction at different time intervals. In ***Procedure I*** synthesis was stopped after 2, 3, 4 and 5 h of heating and stirring, whereas synthesis according to ***Procedure II*** was stopped after 5, 10, 15 and 20 min of sonication without heating. The yield of the obtained PS was calculated from the mass ratio of obtained product (composite particles) and sum of mass of initial reagents. Hence the calculated yield presents the effectiveness of styrene polymerization onto NFC or in other words in PS/NFC composite. As it follows from the Table 2, the optimal reaction times for the ***Procedure I*** and ***Procedure II*** are 3 h and 15 min respectively. The PS yield does not exceed 90 % in both procedures since some part of PS was removed during filtration and washing.

Significant acceleration of PS polymerization in ***Procedure II*** can be explained by several factors related to the inherent sonication properties. A long sonication in ***Procedure II*** led to the better/faster diffusion/distribution of polymerization initiator in the diluted solution. Moreover, H· and HO· radicals formation resulting from sonication of aqueous media [22–24,26] accelerates PS polymerization. According to Y. Jang *et al.* [10], the increase of reduced cellulose quantity in water solution led to the formation of a better Pickering emulsion. A quality of Pickering emulsion (size of polymer droplets) might influence on process rate since polymerization in smaller droplets undergoes faster. A longer time of ultrasonic treatment in ***Procedure II*** leads to more stable and homogeneous Pickering emulsion owing to the better NFC distribution in the volume. Finally, all factors mentioned above resulted in a considerable acceleration of PS polymerization in ***Procedure II***.

FTIR studies of the synthesized composite NFC/PS particles revealed the presence of the both cellulose and PS bands in 600–4000 cm^{-1} (Fig. 1). As it follows from the figure there is no difference between spectra of NFC/PS and NFC/PS/US. In both spectra the bands corresponding to the OH groups and glucose ring oscillations are present indicating presence of NFC in composite materials.

SEM investigations of NFC and synthesized composite particles revealed successful styrene polymerization on cellulose fibrils (see Fig. 2). Again, no considerable difference between NFC/PS and NFC/PS/US samples was observed.

TGA analysis was carried out to study the thermal stability of pure NFC, PS and obtained NFC/PS composites. As it follows from Fig. 3, TGA curves of NFC/PS and NFC/PS/US are identical and have one weight loss step. Despite the fact that cellulose graphitization takes place at 348 °C the maximum decomposition of NFC/PS and NFC/PS/US occurs in 420–430 °C temperature range. Since NFC is covered by PS the decomposition of composite material begins with PS evaporation. It is worth to note that the mass loss of NFC/PS composites is 40 % less than PS's one indicating improved thermal stability of the composites. A probable explanation of this phenomenon could be an increase in ash content due to the addition of cellulose fibres and the intermolecular interaction between polystyrene and cellulose preventing complete PS evaporation and NFC graphitization.

Fig. 4 and Table 3 present results of the mechanical studies of the obtained materials. It is well seen that there is no particular difference between two composites obtained according to ***Procedure I*** and ***Procedure II***. At the same time, one can note that NFC addition to the polymer matrix considerably improved its hardness. Vikers hardness and Martens

Table 1
Intensity of mold fungus development according to ISO 846 ASTM G 21–96.

Score	Description
0	No spore and conidia germination was detected under the microscope
1	Under the microscope you can see germinated spores and slightly developed mycelium
2	Under a microscope, you can see a developed mycelium, possibly sprooning
3	With the naked eye, mycelium and/or sporoderms are barely visible, but clearly visible under a microscope
4	The naked eye can clearly see the development of fungi covering less than 25 % of the test surface
5	The naked eye can clearly see the development of fungi covering more than 25 % of the test surface

Table 2
PS yield (in composite) in ***Procedure I*** and ***Procedure II*** as a function of time.

	time	PS yield, %
Procedure I	2 h	65
	3 h	85
	4 h	86
	5 h	84
Procedure II	5 min	53
	10 min	68
	15 min	85
	20 min	86

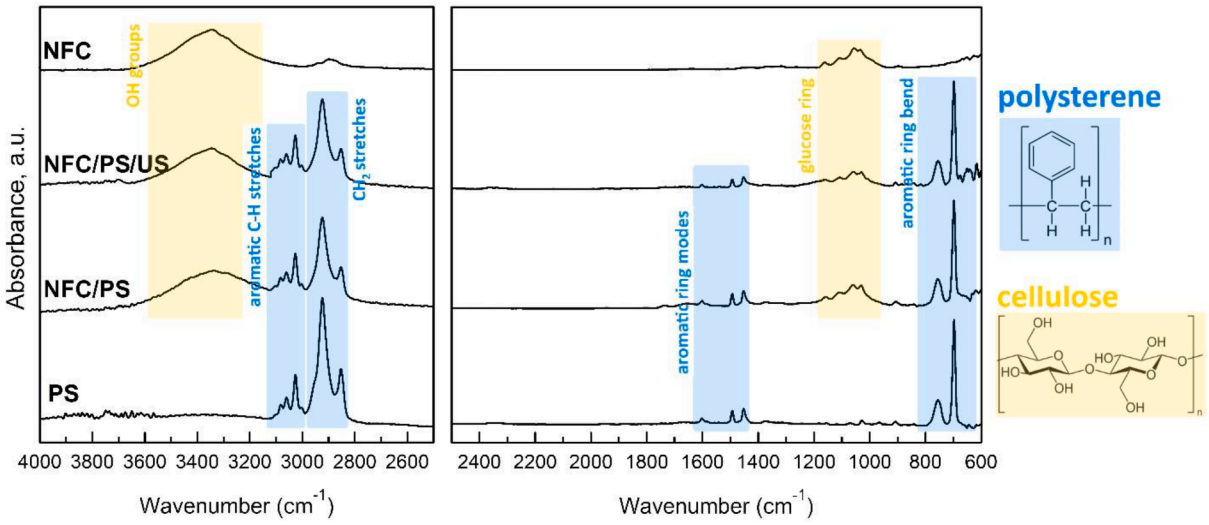

Fig. 1. FTIR spectra of PS, NFC, NFC/PS and NFC/PS/US composites and the structural formulas of PS and cellulose molecules showing the main functional groups in their structure.

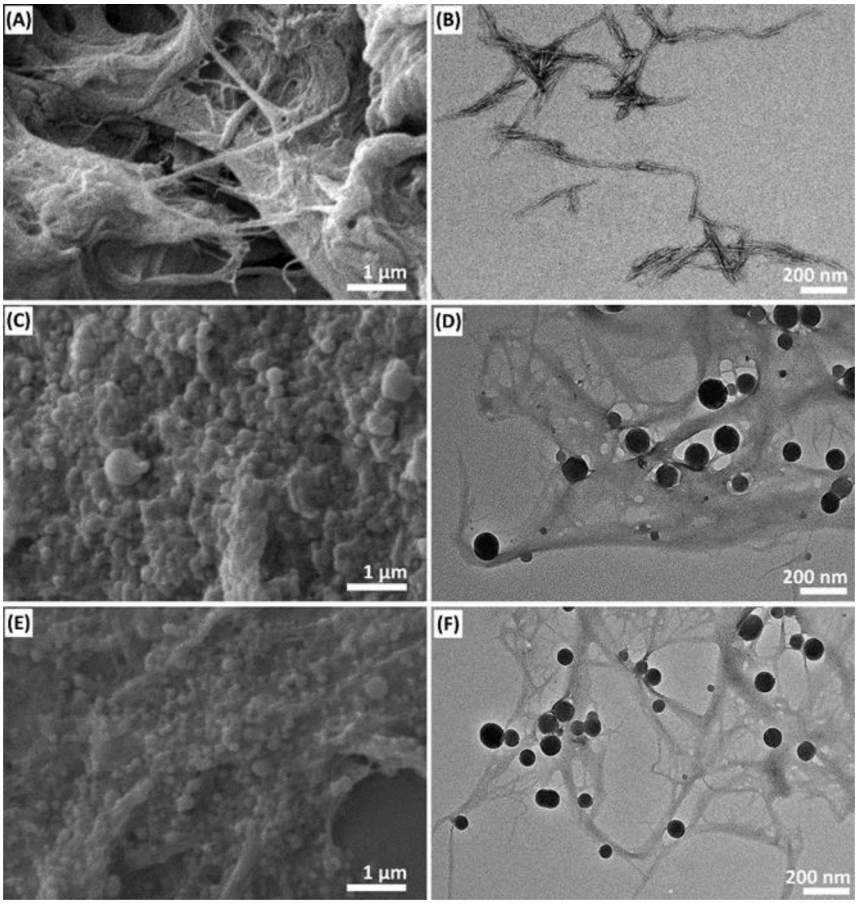

Fig. 2. SEM and TEM micrographs of NFC (A,B), NFC/PS (C,D) and NFC/PS/US (E,F).

hardness of the composites increased by 3 and 2.6 times correspondingly compared to PS matrix according to Table 3. Such a drastic amelioration of composite mechanical properties might be explained, for example, by mechanical percolation effects [32].

It is well known that polymer hydrophobicity is one of clue features for its biodegradability. The composition of plastics determines the hydrophobicity of the polymer surface, which affects feasibility of microorganism adhesion [33]. The hydrophobicity of polystyrene makes them resistant to hydrolysis, however, addition of NFC to polymer matrix alters wetting properties of PS (Fig. 5). A contact angles of NFC/PS and NFC/PS/US are almost identical (74.3° and 74.6° respectively), meanwhile contact angle of PS sample is 94°. Thus, NFC addition to the polymer led to an increase in surface energy of the material owing to presence of hydroxyl groups on the surface of cellulose fibrils, which

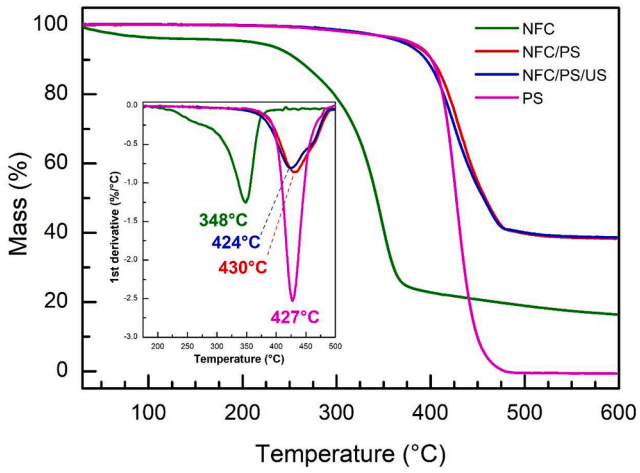

Fig. 3. TGA curves of PS, NFC, NFC/PS, NFC/PS/US; the inset presents the corresponding DTGA curves.

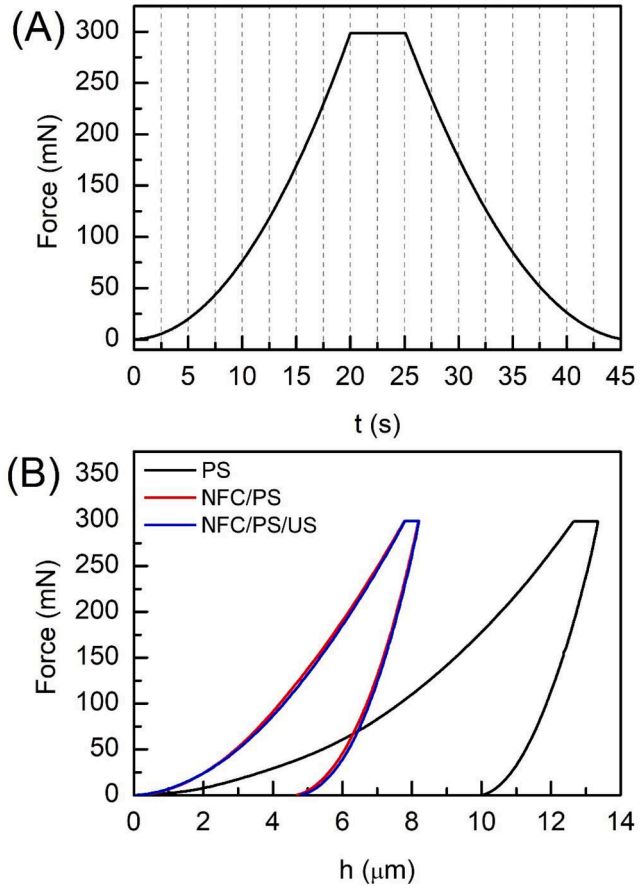

Fig. 4. Dependences of the load force on time (A) and load force on the imprint depth for PS, NFC/PS and NFC/PS/US (B). Pure NFC can not be compared because of its powder form.

Table 3
Hardness tests results for PS, NFC/PS and NFC/PS/US. Pure NFC can not be compared because of its powder form.

Sample	H_M, N/MM^2	H_V
PS	67.5 ± 0.2	8 ± 3
NFC/PS	178 ± 0.3	25 ± 3
NFC/PS/US	177 ± 0.4	25 ± 2

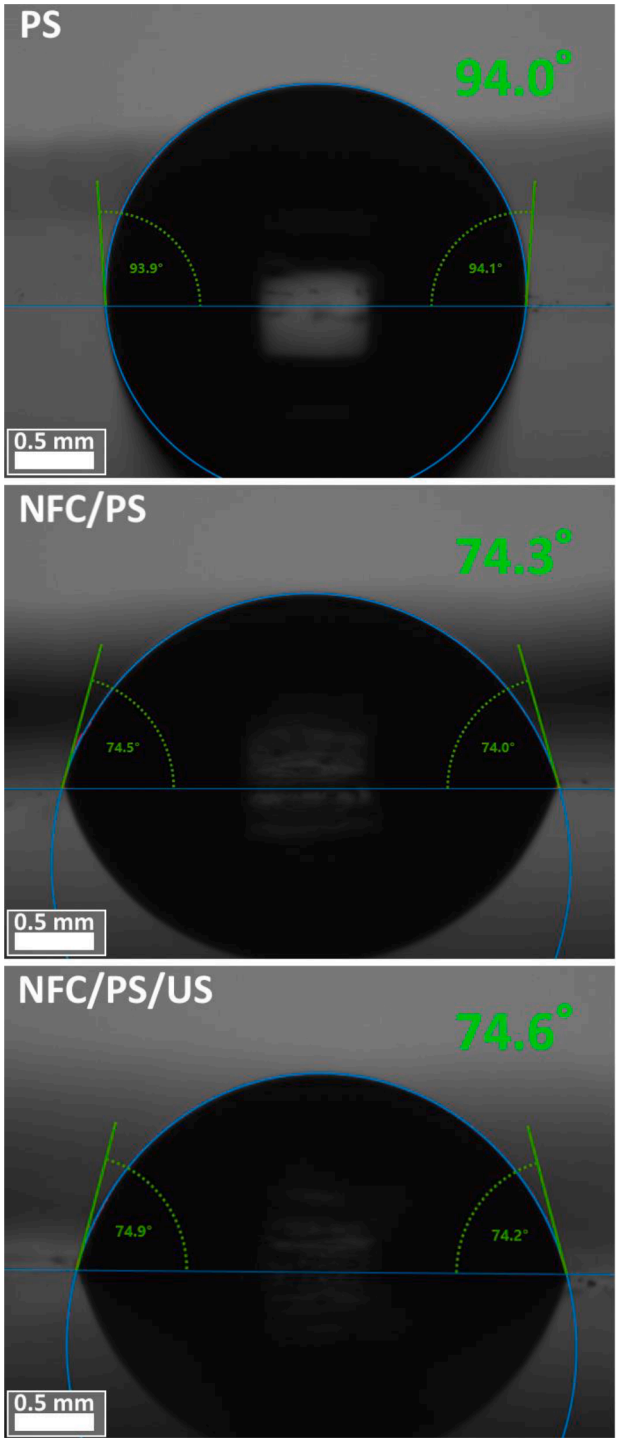

Fig. 5. Sessile drop micrographs for PS, NFC/PS and NFC/PS/US.Scale bar is 0.5 mm. Pure NFC can not be compared because of its powder form.

resulted in a switch of surface wettability from hydrophobic to hydrophilic.

Increased fraction of wetted area of the NFC/PS composites surfaces during wetting and the presence of cellulose fibrils acting as a nutrient source will favor the aqueous media adhesion and microorganisms attachment to the composites as compared to polystyrene.

In obtained NFC/PS composites, cellulose fibres act as a biodegradable matrix that can increase the ability of PS to decompose in the presence of microorganisms. Since fungi are one of the most widespread microorganisms all over the world, a fungal resistance, as well as

fungicidal and fungistatic properties, were studied using microscopic fungi (Fig. 6).

Results of these studies are collected in Table 4. According to our observation, NFC/PS samples possess lower fungal resistance, fungicidal and fungistatic properties than pristine polystyrene, which makes them considerably more biodegradable.

Biodegradation of the polymer materials occurs when the microbial cell (fungi, bacteria, archaea) secrets extracellular enzymes [33]. Low water solubility and high molecular weight of polymers prevent bacteria from direct transport of the material for their cell metabolism and the material cannot be assimilated as a carbon or nitrogen source. Enzymes unable to penetrate into bulk material because of their large size and degrade the polymer chain via hydrolytic mechanisms [34]. So, only the surface biodegradation occurs. The addition of cellulose fibrils to polystyrene makes the NFC/PS composites more susceptible to microbial (fungal) attack. Cellulose acts as a carbon source for fungi feeding which can probably facilitate more degradation of the material; thus decreasing the fungal resistance and increasing its biodegradation ability. Antifungal (fungicidal/fungistatic) properties were also decreased in the presence of cellulose. The surface of all samples does not prevent the growth of fungi on it, however, the largest colonization is observed on the samples with cellulose. The coverage of more than a quarter of the NFC/PS surfaces is revealed as compared to PS.

Table 4
Results of investigation of fungal resistance and fungicidal/fungistatic properties of PS, NFC/PS and NFC/PS/US according to ISO 846 ASTM G 21–96.

Experiment	Fungal growth, scores		
	PS	NFC/PS	NFC/PS/US
Benchmark	0	0	0
Fungal resistance	3	5	5
Fungicidal/fungistatic properties	3	5	5

4. Conclusions

Two methods of NFC/PS composites synthesis via Pickering emulsion polymerization were proposed and compared. It was shown that the sonication of reaction system increases the stability of styrene-water emulsion, accelerates the polymerization and reduces the reaction time from hours to minutes. The yield of PS polymerization in the case of ultrasound treatment is 85 %. A combination of cellulose and polystyrene resulted in improved thermal and mechanical properties which can be accounted for intermolecular interactions between both polymers. Since cellulose is a hydrophilic biopolymer, the wetting performance of NFC/PS composites was changed. The surface of resulted materials became less hydrophobic as compared to pristine polystyrene. Given that cellulose fibrils in the samples is an available carbon source for microorganisms, the attachment of mold fungi on these composites occurs more readily; thus resulting in the significantly higher biodegradability of obtained composites. Application of ultrasound during synthesis results in reduction of the synthetic time (from 3 h to 15 min) and more effective energy consumption lowering reaction temperature from 75 °C to 45 °C.

CRediT authorship contribution statement

K.A. Cherednichenko: Writing – original draft. **A.R. Sayfutdinova:** Data curation, Formal analysis. **A. Kraynov:** Data curation, Formal analysis. **B. Anikushin:** Data curation, Formal analysis. **V. Ignatiev:**

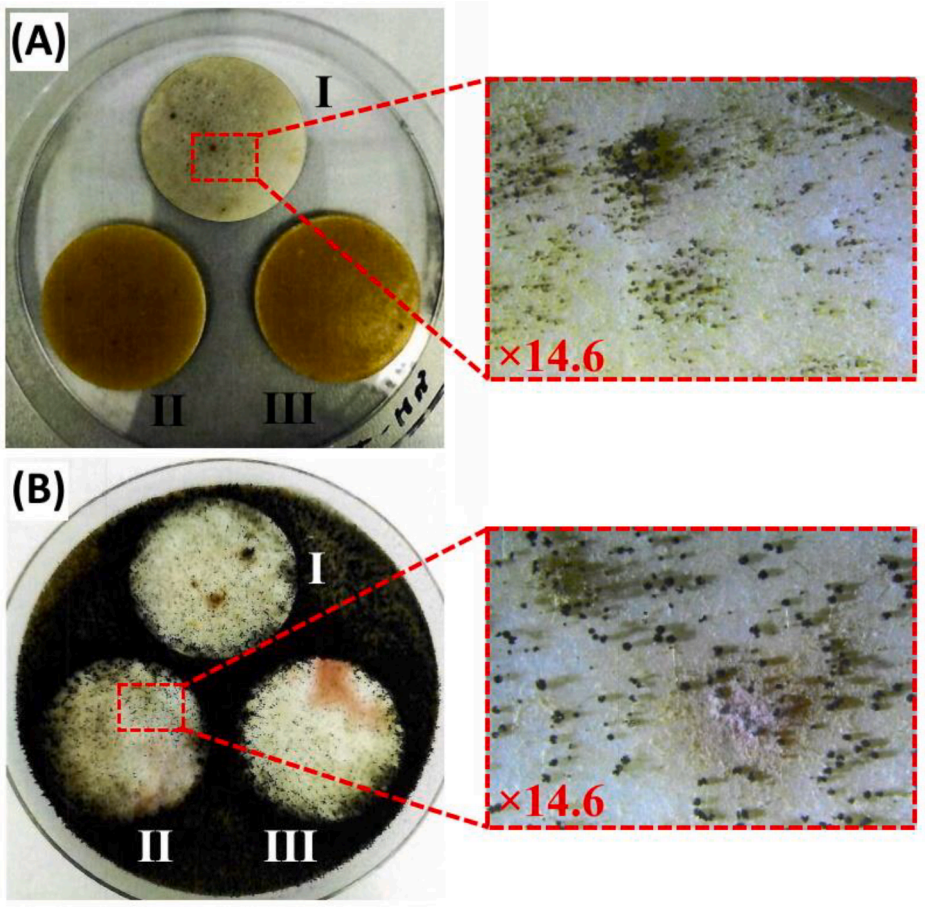

Fig. 6. Microbiological assays of PS (I), NFC/PS (II) and NFC/PS/US (III) using microscopic fungi: fungal resistance (A) and fungicidality/fungistaticity (B).

Methodology. **M.I. Rubtsova:** Methodology. **S.A. Konstantinova:** Investigation. **D.G. Shchukin:** Writing – review & editing. **V.A. Vinokurov:** Writing – review & editing.

Declaration of Competing Interest

The authors declare that they have no known competing financial interests or personal relationships that could have appeared to influence the work reported in this paper.

Data availability

The authors do not have permission to share data.

Acknowledgement

The authors acknowledge support from RSC grant IEC\NSFC \181714 and RSF grant (#19-79-30091).

Appendix A. Supplementary data

Supplementary data to this article can be found online at https://doi.org/10.1016/j.ultsonch.2022.106180.

References

[1] Y. Nishiyama, Structure and properties of the cellulose microfibril, J. Wood Sci. 55 (4) (2009) 241–249, https://doi.org/10.1007/s10086-009-1029-1.
[2] S.J. Einchhorn, A. Dufresne, M.M. Aranguren, J.R. Capadona, S.J. Rowan, C. Weder, S. Veigel, Current international research into cellulose nanofibres and composites, J. Mater. Sci. 45 (2010) 1–33, https://doi.org/10.1007/s10853-009-3874-0.
[3] I. Siró, D. Plackett, Microfibrillated cellulose and new nanocomposite materials: a review, Cellulose 17 (3) (2010) 459–494, https://doi.org/10.1007/s10570-010-9405-y.
[4] B.L. Peng, N. Dhar, H.L. Liu, K.C. Tam, Chemistry and applications of nanocrystalline cellulose and its derivatives: a nanotechnology perspective, Can. J. Chem. Eng. 89 (5) (2011) 1191–1206, https://doi.org/10.1002/cjce.20554.
[5] K. Missoum, M. Belgacem, J. Bras, Nanofibrillated Cellulose Surface Modification: A Review, Materials 6 (5) (2013) 1745–1766.
[6] M. Mariano, C. Chirat, N. El Kissi, A. Dufresne, Cellulose nanocrystals and related nanocomposites: review of some properties and challenges, J. Polym. Sci. B: Polym. Phys. 52 (12) (2014) 791–806, https://doi.org/10.1002/polb.23490.
[7] N. Tamura, K. Ban, S. Takahashi, T. Kasemura, S. Obuchi, Application of Poly (acetic Acid)–Based Graft Copolymer as a Compatibilizer for Poly (L-lactic Acid)/Poly (butylenesuccinate) Blend System, J. Adhes. 82 (4) (2006) 355–373, https://doi.org/10.1080/00218460600683787.
[8] A. Dufresne, D. Dupeyre, M. Paillet, Lignocellulosic flour-reinforced poly (hydroxybutyrate-co-valerate) composites, J. Appl. Polym. Sci. 87 (8) (2003) 1302–1315, https://doi.org/10.1002/app.11546.
[9] A. Sorrentino, G. Gorrasi, V. Vittoria, Potential perspectives of bio-nanocomposites for food packaging applications, Trends Food Sci. Technol. 18 (2) (2007) 84–95, https://doi.org/10.1016/j.tifs.2006.09.004.
[10] Y. Jiang, Y. Zhang, L. Ding, A. Joshua, B. Wang, X. Feng, Z. Chen, Z. Mao, X. Sui, Regenerated cellulose-dispersed polystyrene composites enabled via Pickering emulsion polymerization, Carbohydr. Polym. 223 (2019), 115079, https://doi.org/10.1016/j.carbpol.2019.115079.
[11] L. Song, Z. Wang, M.E. Lamm, L. Yuan, C. Tang, Supramolecular polymer nanocomposites derived from plant oils and cellulose nanocrystals, Macromol. 50 (19) (2017) 7475–7483, https://doi.org/10.1021/acs.macromol.7b01691.
[12] Y. Zhang, J. Wu, B. Wang, X. Sui, Y.I. Zhong, L. Zhang, Z. Mao, H. Xu, Cellulose nanofibril-reinforced biodegradable polymer composites obtained via a Pickering emulsion approach, Cellulose 24 (8) (2017) 3313–3322.
[13] C. Bonini, L. Heux, J.Y. Cavaillé, P. Lindner, C. Dewhurst, P. Terech, Rodlike cellulose whiskers coated with surfactant: a small-angle neutron scattering characterization, Langmuir 18 (8) (2002) 3311–3314, https://doi.org/10.1021/la015511t.
[14] N. Lin, J. Huang, P.R. Chang, J. Feng, J. Yu, Surface acetylation of cellulose nanocrystal and its reinforcing function in poly (lactic acid), Carbohydr. Polym. 83 (4) (2011) 1834–1842, https://doi.org/10.1016/j.carbpol.2010.10.047.
[15] J. George, M.S. Sreekala, S. Thomas, A review on interface modification and characterization of natural fiber reinforced plastic composites, Polym. Eng. Rev. 41 (9) (2001) 1471–1485, https://doi.org/10.1002/pen.10846.
[16] B. Wang, M. Sain, K. Oksman, Study of structural morphology of hemp fiber from the micro to the nanoscale, Appl. Compos. Mater. 14 (2) (2007) 89–103, https://doi.org/10.1007/s10443-006-9032-9.
[17] Q. Cheng, S. Wang, T.G. Rials, S.H. Lee, Physical and mechanical properties of polyvinyl alcohol and polypropylene composite materials reinforced with fibril aggregates isolated from regenerated cellulose fibers, Cellulose 14 (6) (2007) 593–602, https://doi.org/10.1007/s10570-007-9141-0.
[18] Z. Wang, L. Yuan, C. Tang, Sustainable Elastomers from Renewable Biomass, Acc. Chem. Res. 50 (7) (2017) 1762–1773.
[19] A.J.F. Carvalho, E. Trovatti, C.A. Casale, Polystyrene/cellulose nanofibril composites: fiber dispersion driven by nanoemulsion flocculation, J. Mol. Liq. 272 (2018) 387–394, https://doi.org/10.1016/j.molliq.2018.09.089.
[20] Y. Zhang, Y. Jiang, L. Han, B. Wang, H. Xu, Y. Zhong, L. Zhang, Z. Mao, X. Sui, Biodegradable regenerated cellulose-dispersed composites with improved properties via a pickering emulsion process, Carbohydrate polymers 179 (2018) 86–92, https://doi.org/10.1016/j.carbpol.2017.09.065.
[21] A.S. Ostroski, R.B. Stambaugh, Emulsion polymerization with ultrasonic vibration, J. Appl. Phys. 21 (6) (1950) 478–482, https://doi.org/10.1063/1.1699689.
[22] P. Kruus, Polymerization resulting from ultrasonic cavitation, Ultrasonics 21 (5) (1983) 201–204, https://doi.org/10.1016/0041-624X(83)90041-0.
[23] P. Kruus, M. O'Neill, D. Robertson, Ultrasonic initiation of polymerization, Ultrasonics 28 (5) (1990) 304–309, https://doi.org/10.1016/0041-624X(90)90036-N.
[24] G.J. Price, D.J. Norris, P.J. West, Polymerization of methyl methacrylate initiated by ultrasound, Macromol. 25 (24) (1992) 6447–6454, https://doi.org/10.1021/ma00050a010.
[25] G.J. Price, Ultrasonically enhanced polymer synthesis, Ultrason. Sonochem. 3 (3) (1996) S229–S238, https://doi.org/10.1016/S1350-4177(96)00031-4.
[26] Y. Kojima, S. Koda, H. Nomura, Effect of ultrasonic frequency on polymerization of styrene under sonication, Ultrason. Sonochem. 8 (2) (2001) 75–79, https://doi.org/10.1016/S1350-4177(00)00064-X.
[27] A.A. Novikov, B.M. Anikushin, D.A. Petrova, S.A. Konstantinova, V.B. Mel'nikov, V.A. Vinokurov, Acid and oxidative treatment of raw material for the production of nanofibrillar cellulose, Chem Technol Fuels Oils 54 (5) (2018) 564–568.
[28] C.A. Schneider, W.S. Rasband, K.W. Eliceiri, NIH Image to ImageJ: 25 years of image analysis, Nat. Methods 9 (7) (2012) 671–675, https://doi.org/10.1038/nmeth.2089.
[29] J. Schindelin, I. Arganda-Carreras, E. Frise, V. Kaynig, M. Longair, T. Pietzsch, S. Preibisch, C. Rueden, S. Saalfeld, B. Schmid, J.-Y. Tinevez, D.J. White, V. Hartenstein, K. Eliceiri, P. Tomancak, A. Cardona, Fiji: an open-source platform for biological-image analysis, Nat. Methods 9 (7) (2012) 676–682, https://doi.org/10.1038/nmeth.2019.
[30] X. Jia, R. Xu, W. Shen, M. Xie, M. Abid, S. Jabbar, P. Wang, X. Zeng, T. Wu, Stabilizing oil-in-water emulsion with amorphous cellulose, Food Hydrocoll. 43 (2015) 275–282, https://doi.org/10.1016/j.foodhyd.2014.05.024.
[31] C. Tang, S. Spinney, Z. Shi, J. Tang, B. Peng, J. Luo, K.C. Tam, Amphiphilic cellulose nanocrystals for enhanced Pickering emulsion stabilization, Langmuir 34 (43) (2018) 12897–12905, https://doi.org/10.1021/acs.langmuir.8b02437.
[32] A. Kaboorani, B. Riedl, P. Blanchet, M. Fellin, O. Hosseinaei, S. Wang, Nanocrystalline cellulose (NCC): A renewable nano-material for polyvinyl acetate (PVA) adhesive, Eur. Polym. J. 48 (11) (2012) 1829–1837, https://doi.org/10.1016/j.eurpolymj.2012.08.008.
[33] B.T. Ho, T.K. Roberts, S. Lucas, An overview on biodegradation of polystyrene and modified polystyrene: the microbial approach, Crit. Rev. Biotechnol. 38 (2) (2018) 308–320, https://doi.org/10.1080/07388551.2017.1355293.
[34] T. Artham, M. Doble, Biodegradation of aliphatic and aromatic polycarbonates, Macromol. Biosci. 8 (1) (2008) 14–24, https://doi.org/10.1002/mabi.200700106.